

# UC Berkeley

## UC Berkeley Previously Published Works

### Title

A Non-Volatile Surface Tension-Driven Electrochemical Liquid Metal Actuator

### Permalink

<https://escholarship.org/uc/item/2mf7z6hx>

### Authors

Chen, Xiaohang

Wang, Zihan

Yue, Wei

[et al.](#)

### Publication Date

2024-01-25

### DOI

10.1109/mems58180.2024.10439595

### Copyright Information

This work is made available under the terms of a Creative Commons Attribution License, available at <https://creativecommons.org/licenses/by/4.0/>

Peer reviewed

# A NON-VOLATILE SURFACE TENSION-DRIVEN ELECTROCHEMICAL LIQUID METAL ACTUATOR

Xiaohang Chen<sup>1</sup>, Zihan Wang<sup>1,2</sup>, Wei Yue<sup>1</sup>, Peisheng He<sup>\*1</sup>, and Liwei Lin<sup>1</sup>

<sup>1</sup>University of California, Berkeley, USA and

<sup>2</sup>Tsinghua-Berkeley Shenzhen Institute, Tsinghua University, CHINA.

## ABSTRACT

We present a surface-tension driven electrochemical liquid metal (LM) actuator without the gas-producing side-reaction and capable of fabrication/operation in ambient air for practical applications. A hybrid supercapacitor is introduced to inhibit the common counter electrode side reactions, and the use of quasi-solid-state ionic hydrogel instead of liquid electrolyte further enables non-volatile operations. A 2×4 LM droplet array is demonstrated to actuate by a low driving voltage of 3.5 V for a maximum force of ~8.5 mN and a displacement of 0.56 mm in only 1.75 s. With the favorable scaling law of surface tension, further miniaturization could provide new opportunities in applications such as micro-robots, microfluidics, soft robots, and so on.

## KEYWORDS

Liquid Metal; Surface Tension; Electrochemical Actuator; Hydrogel.

## INTRODUCTION

Surface tension plays an important role in miniaturized systems as the scaling law favors its relative significance over other forces such as gravity, magnetic, and structural stiffness [1]. As such, surface tension effects have induced process issues in microfabrication such as stiction but also provided opportunities in using the surface tension to drive microdevices, such as those based on electrowetting-on-dielectric (EWOD) [2], electrocapillary [3], and continuous electrowetting (CEW) mechanism [4], ... etc. Recently, giant outputs by the switching of surface tension from ~500 mN/m to near zero have been exploited to artificial muscles and linear actuators by the reversible redox reaction at the surface of eutectic gallium–indium (EGaIn) droplets [5], [6]. Compared to other actuation mechanisms such as piezoelectric, electrostatic (e.g., dielectric elastomer actuator), and shape memory alloys (SMA), this scheme provides attractive features of low-voltage operation (as low as ~0.5 V), high energy density at small length scales, and good operation frequency (~5 Hz) [6], [7]. However, current liquid metal (LM) actuators rely on using liquid electrolyte for ion transports, which limits the operation environments and further miniaturization. Moreover, side reactions lead to the generation of gas bubbles on both working and counter electrodes and constraint possible practical applications.

Herein, a quasi-solid ionic hydrogel is proposed to form a hybrid supercapacitor without liquid electrolyte, as shown in **Figure 1**. The reversible surface tension changes at the liquid metal surface result in the lateral movements of the top electrode. The liquid metal droplet is oxidized when a positive voltage is applied to reduce its surface tension. Conversely, a negative voltage reduces the

oxidized layer to increase the surface tension. Laser-induced graphene (LIG) is utilized as an electrical double layer capacitive (EDLC) electrode, forming a hybrid supercapacitor with the LM droplet on the working electrode. When the working electrode goes through the reversible redox reaction of Ga/Ga<sub>2</sub>O<sub>3</sub>, the counter electrode stores charge in a capacitive manner without the gas-producing water electrolysis process.

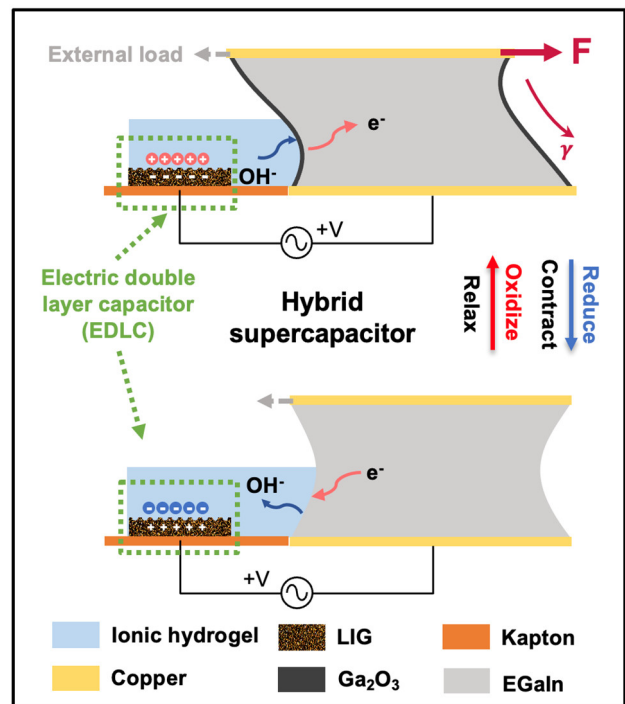


Figure 1: Mechanism: The liquid metal actuator where the thin surface gallium oxide layer reduces surface tension while reduced gallium contributes to high surface tension. During redox reactions, electric double layers are formed on the LIG counter electrodes.

## RESULTS AND DISCUSSION

### Material Synthesis of electrode and electrolytes

The ionic hydrogel, employed as the electrolyte within the system, is synthesized by combining polyvinyl alcohol (PVA) and ethylene glycol (EG) with weight percentages of 8.2% and 3.0%, respectively, in water. To maintain an alkaline environment within the hydrogel, potassium hydroxide (KOH) is added at a weight percentage of 0.75%. Additionally, lithium chloride (LiCl) is incorporated at a weight percentage of 2.5% as the electrolyte salt and the water absorber from the surrounding environment. The resulting solution is subjected to a temperature of 70°C in an oil bath for a duration of 4 hours. LIG, utilized as an electrode for the electric double-layer capacitor (EDLC), is produced by utilizing a laser cutter (Omtech™, SH-G3020) in ablation mode, with parameters set to a speed of 500

mm/s and a power of 8W. This laser ablation process is performed on a 50  $\mu\text{m}$ -thick polyimide (PI) film.

### Long-term operation performance

The non-volatile operation of the system is achieved by first eliminating the side reaction of the electrolyte. In prior works, copper is utilized as the counter electrode. During the electrochemical modulation of surface tension effect, hydrogen gas is generated at the working electrode and oxygen at the counter electrode. This is also observed in **Figure 2a**, where an electrochemical cell consisting of a single droplet of LM (20  $\mu\text{L}$ ) and copper electrode is immersed in 1.5M KOH solution. When a 4V amplitude sinusoidal wave is applied, noticeable bubble generation is observed on the electrode. These bubbles can degrade the performance as they accumulate on the liquid metal surface. At smaller scales, bubbles may block the ionic connection and stop the reaction. To address this issue, we introduce the LIG at the counter electrode to form an EDLC-like architecture. To establish a comparative analysis with prior works, we replicated the identical experimental setup but replaced the copper electrode with a graphene electrode (**Figure 2b**). During operation, the reversible redox reactions of Ga/Ga<sub>2</sub>O<sub>3</sub> occur at the working electrode. At the counter electrode, the charge is stored in a capacitive manner thanks to the large specific area of LIG. As a result, the electrolysis of electrolyte is suppressed, thus preventing bubble generations.

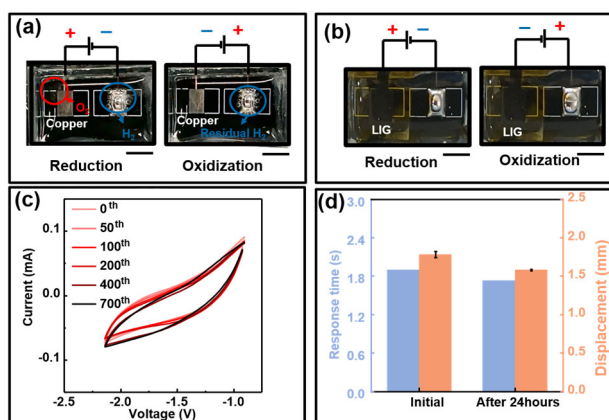


**Figure 2:** a. The production of bubbles in an LM-based actuator using 1.5M KOH liquid electrolyte and copper electrode. b. No bubbles with the LIG electrode. Scale bars, 5 mm. c. The cyclic voltammetry measurement of the device (scan rate 400mV/s). d. Comparison of the initial output displacement and response time of the 2x4 system (left) and after 24 hours (right).

Subsequently, the KOH solution is substituted with a polyvinyl alcohol-based ionic hydrogel. Under a negative potential, oxidation of the liquid metal occurs, while under a positive potential, reduction takes place. Based on the redox potential of gallium, a cyclic voltammetry (CV) test between -0.9 V and -2.1 V is performed using an electrochemical workstation to evaluate the device's long-term stability. After 700 cycles over the course of one hour, the CV curves remain nearly unchanged, and a good

capacitance retention of approximately 92% (**Figure 2c**) is obtained, indicating excellent long-term stability. Additionally, the device's output and response time remained consistent after exposure to the ambient environment (relative humidity of ~50%) for 24 hours (**Figure 2d**), highlighting the ambient stability of the non-volatile design based on the hydrogel electrolyte.

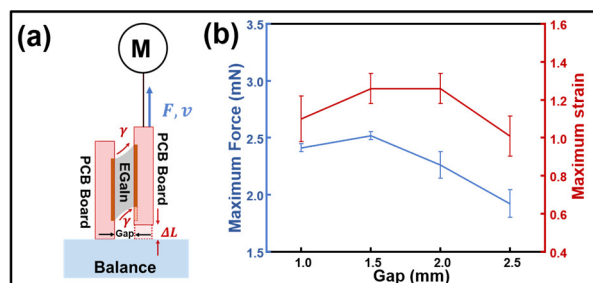


**Figure 3:** a. The test setup for the surface tension-driven actuator with one part fixed on a balance and the other part on a stepper motor. b. The force  $F$  and strain  $\Delta L/L$  output versus gap distance between two PCB boards.

### Force and Strain from a Single Droplet

A key consideration in using the LM droplet as an actuator is its susceptibility to rupture under excessive stretching. The behavior of the liquid is governed by surface free energy, and instability arises when the liquid tends to separate to minimize its potential energy. To evaluate the theoretical limits of stress-strain output and determine the optimal design for the operating range in LM actuators, we investigate the output characteristics of a single LM droplet, as shown in **Figure 3a**. In the experiment, a 20  $\mu\text{L}$  LM droplet is deposited on the surface of two parallel boards with exposed copper surfaces, each measuring 3 mm  $\times$  5 mm. One board is fixed to a balance, while the other is connected to a stepper motor. The stepper motor operates at a velocity of 0.35 mm/s, causing the droplet to undergo elongation until rupture. By varying the gap between the two boards from 1mm to 2.5 mm, the rupture time of the droplet is measured. The maximum shear strain is calculated from the data and the force at which the rupture occurs is recorded by the balance (**Figure 3b**). Video footage is analyzed to extract the necessary information. The results reveal that a single LM droplet exhibits a maximum force output of 2.5 mN and a strain of 125% at a 2.5 mm gap. This corresponds to a work density (W/V) of 750 J/m<sup>3</sup>, surpassing that of electrocapillarity systems (1-100 J/m<sup>3</sup>).

### Array Integration and Actuation Performance

In order to achieve higher output force, individual LM droplets can be integrated into an array. The shearing mode of actuation allows such scaling to be achieved by simply introducing more units on the same plane in parallel. Herein, as a demonstration, a pair of printed circuit boards (PCBs) are designed to hold a 2 by 4 LM droplet array. The layout of the PCBs is shown in **Figure 4a**, where the dimension of each copper pixel on the boards is 3 $\times$ 5 mm. To prevent unexpected joining of LM droplets, the horizontal and vertical gap between two adjacent pixels is set to be 8 mm and 7 mm, respectively. Note that the 8-wire

connector on the left end of the stator PCB is connecting 8 pixels individually.

Then, we assemble the arrayed actuator (**Figure 4b**) with the following steps. First, a 50  $\mu\text{m}$  thick PI film is coated on the stator PCB. Then a laser cutter (Omtech<sup>TM</sup>, SH-G3020) is used to cut out polyimide above each copper pixel in the cutting mode (10 mm/s, 20 W power) and patterns LIG electrode by the ablation mode (500 mm/s, 8 W power). Afterward, the ionic hydrogel is patterned above the PI film by a stencil printing process and left overnight until the water concentration of the hydrogel reaches the equilibrium with the ambient environment. Subsequently, a syringe is used to precisely dispense a 20- $\mu\text{L}$  EGaIn droplets on each exposed copper pixel. Finally, 3 mm in diameter stainless steel bearing balls are placed on both sides of PCB grooves, and a slider PCB is placed above. Since the LM droplet will wet copper pixels on the slider PCB, the stator PCB and slider PCB align autonomously in the reduced state. During operation, the 8 connectors on the stator PCB are tied to the positive terminal of the waveform generator, and the negative terminal is connected to the LIG electrode, and a voltage is applied to control the redox reaction on the LM droplets.

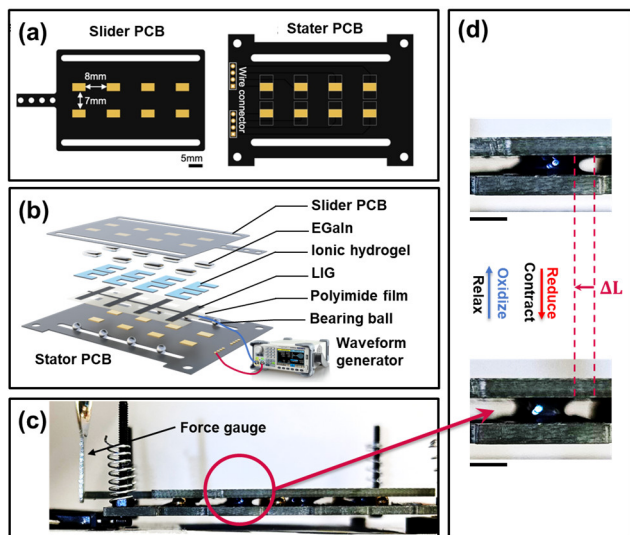


**Figure 4:** Integration of arrayed actuator: (a) Layout of PCBs for array integration. (b) The exploded view of the actuator assembly. (c) Optical photos of the actuation results in hydrogel electrolyte by  $-3.5\text{V}$  and  $0\text{V}$  for oxidized (top) and reduced state (bottom). Scale bars, 5mm. (d) An optical photo of the setup.

To evaluate the force and strain outputs of the integrated device in response to the temporal variation of current and voltage, a comprehensive test setup is established. Given that the force outputs are in the mN range, a high-precision spring gauge is affixed to one side of the slider PCB, while the stator PCB is mounted on the table (**Figure 4c**). As illustrated in **Figure 4d**, the oxidation-reduction process of gallium changes the surface tension of the LM droplet to result in the movement of the slider PCB. Herein, the input waveform generated by the signal generator consists of a step voltage from  $0\text{V}$  to  $-3.5\text{V}$ . In the oxidation stage ( $0\text{V}$ ), an oxide layer forms on the LM surface, and the surface tension is low. Conversely, when fully reduced (at  $-3.5\text{V}$ ), the surface tension of the

liquid metal reaches its maximum to result in the horizontal movement of the upper plate for an output reading to the spring gauge that represents the force output of the arrayed actuator. To measure the force, a slow-motion video is recorded at 240 frames per second, allowing for the reading of the gauge pointer. Subsequently, an edge recognition algorithm is implemented in MATLAB to accurately extract the orientation of the gauge pointer over time, thereby revealing the variations in force. Displacement is also quantified by tracking the movement of a specific point on the slider PCB.

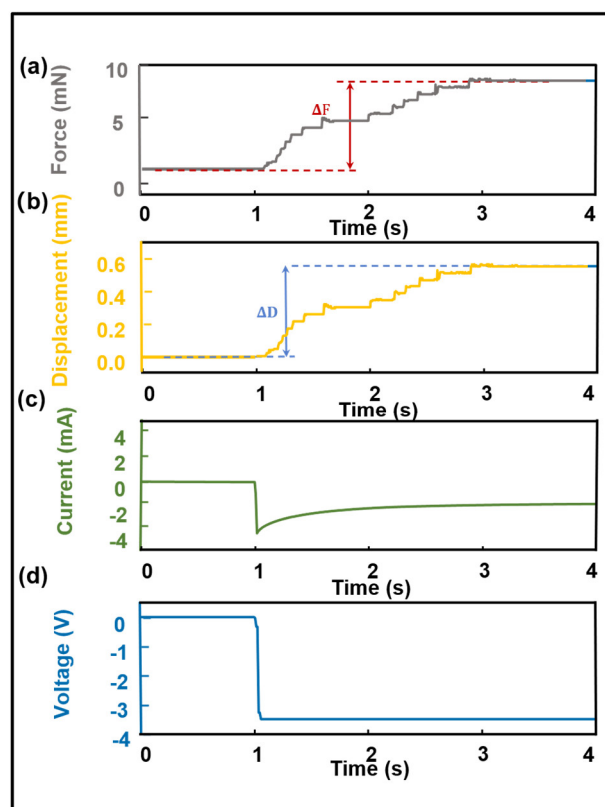


**Figure 5:** Measured a) force output, b) displacement, and c) current response of a  $2 \times 4$  LM system in response to a  $-3.5\text{V}$  voltage change.

**Figure 5** depicts the output force, displacement, and the corresponding input current of the array actuator. In the zero-output state, with an applied voltage of  $0\text{V}$ , the actuator remains in its initial configuration. When the voltage is stepped up to  $-3.5\text{V}$ , the displacement of the slider board is initiated almost instantaneously. Notably, the maximum displacement achieved during the actuation reaches  $0.56\text{mm}$ , corresponding to a maximum force output of approximately  $8.5\text{mN}$ . By analyzing the relationship between the input voltage and the resulting force output, the actuation response time is determined to be approximately  $1.75\text{s}$ . It is worth mentioning that other electrochemical-driven actuators typically require several seconds to hours for the actuation.

The maximum current drawn from the generator during actuation is measured at  $2.5\text{mA}$ . Additionally, the energy density, calculated as the product of force and displacement divided by volume, is found to be  $118\text{J/m}^3$ . The favorable scaling law ( $W/V \propto L^{-1}$ ) indicates a higher theoretical

energy density of approximately 750 kJ/m<sup>3</sup> for microscale systems [6], highlighting the potential for achieving significant energy density in miniaturized systems.

## CONCLUSION

In summary, this paper presents a surface-tension driven electrochemical LM actuator that effectively eliminates the gas-producing side reaction, allowing for its practical fabrication and operation in ambient air. The incorporation of a hybrid supercapacitor architecture effectively addresses the issue of hydrogen byproducts resulting from the water electrolysis process, mitigating the counter electrode side reaction problems. As such, a quasi-solid-state ionic hydrogel can be utilized as the electrolyte, which enables long-term and non-volatile operations. As a demonstration, an integrated actuator consisting of a 2×4 array of LM droplets is fabricated to achieve shear-mode actuation in the air. Notably, the commercial PCB process is utilized to fabricate the substrate, and LIG electrodes are conveniently patterned using a laser engraver, highlighting the overall simplicity and scalability of the fabrication process. The LM actuator realizes stable operation in air and achieves comparable performance as other LM actuators that operates in a liquidous electrolyte bath, which significantly expands its application scenarios. Moreover, leveraging the advantageous scaling law of surface tension, further miniaturization of this technology holds immense promise for novel applications in micro robots, microfluidics, soft robots, and other related domains.

## ACKNOWLEDGEMENTS

This work is in part supported by the Berkeley Sensor and Actuator Center. The authors thank Megan Teng for kindly helping with the initial prototyping process.

## REFERENCES

- [1] R.R.A. Syms, E.M. Yeatman, V.M. Bright, and G.M. Whitesides, "Surface tension-powered self-assembly of microstructures - the state-of-the-art", *J. Microelectromech. Syst.*, vol. 12, no. 4, pp. 387–417, Aug. 2003.
- [2] I. Moon and J. Kim, "Using EWOD (electrowetting-on-dielectric) actuation in a micro conveyor system", *Sens Actuators A Phys*, vol. 130–131, pp. 537–544, Aug. 2006.
- [3] M. Zimmermann, H. Schmid, P. Hunziker, and E. Delamarche, "Capillary pumps for autonomous capillary systems", *Lab Chip*, vol. 7, pp. 119–125, 2007.
- [4] Kwang-Seok Yun, Il-Joo Cho, Jong-Uk Bu, Chang-Jin(CJ) Kim, and Euisik Yoon, "A surface-tension driven micropump for low-voltage and low-power operations", *J. Microelectromech. Syst.*, vol. 11, no. 5, pp. 454–461, Oct. 2002.
- [5] Jian Shu, Du-An Ge, Erlong Wang, Hongtai Ren, Tim Cole, Shi-Yang Tang, Xiangpeng Li, Xiangbo Zhou, Rongjie Li, Hu Jin, Weihua Li, Michael D. Dickey, and Shiwu Zhang, "A Liquid Metal Artificial Muscle", *Advanced Materials*, vol. 33, no. 43, 2103062, Oct. 2021.

[6] J. Liao and C. Majidi, "Muscle-Inspired Linear Actuators by Electrochemical Oxidation of Liquid Metal Bridges", *Advanced Science*, vol. 9, no. 26, Sep. 2022.

[7] J. Liao, C. Majidi, and M. Sitti, "Liquid Metal Actuators: A Comparative Analysis of Surface Tension Controlled Actuation", *Advanced Materials*, 2300560, Jun. 2023.

## CONTACT

\*P. He, tel: +1-510-345-8380; [hopsoshe@berkeley.edu](mailto:hopsoshe@berkeley.edu)